Histol Histopathol (2016) 31: 793-805

http://www.hh.um.es

Histology and Histopathology

From Cell Biology to Tissue Engineering

Protective function of pirfenidone and everolimus on the development of chronic allograft rejection after experimental lung transplantation

M. von Suesskind-Schwendi[1], E. Heigel[2], S. Pfaehler[2], A. Haneya[3], C. Schmid[1], S.W. Hirt[1] and K. Lehle[1]

[1]Department of Cardiothoracic Surgery, [2]Institute of Pathology, University Medical Center, Regensburg and [3]Department of Immunology, University Hospital of Schleswig-Holstein, Campus Kiel, Kiel, Germany

Summary. Long-term survival of lung allografts is limited by chronic rejection (CR). Oxidative stress (OxS) plays a central role in the development of CR. We investigated the influence of pirfenidone (alone or in combination with everolimus) on OxS and CR.

A rat model of left lung allo-transplantation (F344-to-WKY) was used to evaluate the effects of pirfenidone alone [0,85% in chow from postoperative day (POD) -3 to 20/60] and in combination with everolimus [2,5 mg/kg bw daily from POD 7 to 20/60]. Allografts of non-treated animals, everolimus treated animals and right, non-transplanted lungs were used as references. Immunohistology of myeloperoxidase (MPO), haemoxygenase-1 (HO-1), iron and platelet-derived-growth-factor-receptor-alpha (PDGFR-a) were performed.

On POD 20, all groups showed severe acute rejection (ISHLT A3-4/B1R-B2R). Groups treated with pirfenidone showed a lower interstitial inflammatory infiltration and a lower participation of highly fibrotic degenerated vessels (ISHLT-D2R). In the long term follow up (POD 60), pirfenidone alone significantly reduced chronic airway rejection (ISHLT-C; $p \leq 0.05$), interstitial fibrosis (IF; $p \leq 0.05$), content of collagen ($p \leq 0.05$), expression of PDGFR-a ($p \leq 0.05$) and the deposition of iron ($p \leq 0.05$). All groups treated with pirfenidone showed a high expression of the cytoprotective enzyme HO-1 ($p \leq 0.05$). The additional application of everolimus resulted in a significant decrease of chronic airway rejection (ISHLT-C; $p \leq 0.05$), vasculopathy (ISHLT; $p \leq 0.05$) and IF ($p \leq 0.05$).

In conclusion, early application of pirfenidone inhibited the progression of CR by its anti-fibrotic and anti-oxidative properties. The additional application of an m-TOR-inhibitor increased the anti-fibrotic effects of pirfenidone which resulted in a reduction of CR after experimental LTx.

Key words: Lung transplantation, Rat, Chronic rejection, Pirfenidone, Everolimus

Offprint requests to: M.v. Süßkind, Department of Cardiothoracic Surgery, University Hospital of Schleswig-Holstein/Campus Kiel, Kiel, Germany. e-mail: marietta.suesskind-von@klinik.uni-regensburg.de

DOI: 10.14670/HH-11-712

Introduction

Lung transplantation has become an effective clinical treatment for patients with end-stage pulmonary diseases. However, in spite of improved surgical techniques, donor organ preservation solutions and immunosuppression regimes, chronic allograft rejection (CR), is a severe complication in the form of obliterative bronchiolitis (BO) and vasculopathy and limits long-term allograft survival (Scott et al., 2005). Multiple factors seem to be responsible for the development of CR (Weigt et al., 2013). Besides acute rejections (AR) and lymphocytic bronchiolitis, oxidative stress plays a central role in the development of CR (Riise et al., 1998; Mallol et al., 2011). In proposed pathogenic mechanisms of pulmonary fibrosis, the development of fibrotic disorders and therefore also of CR centers on the hypothesis that in response to injury, the damaging effects of oxidants on the lung architecture lead to

fibroblast activation and collagen production triggered by fibrotic growth factors (such as PDGF) (Ray et al., 2003; Gao et al., 2008; Todd et al., 2012; Cheresh et al., 2013).

Pirfenidone (5-methyl-1-phenylpyridin-2-one) is an anti-fibrotic agent. Its anti-fibrotic (McKane et al., 2004; Liu et al., 2005; Zhou et al., 2005), anti-inflammatory (Liu et al., 2005) and anti-oxidative stress (Liu et al., 2005) properties have already been demonstrated in several animal models of AR and of obliterative airway disease (OAD) of the lung. The role of pirfenidone in reducing oxidative stress has also been confirmed in in-vivo (Mitani et al., 2008) and *in vitro* studies of other organs such as kidney (Ji et al., 2013) and neuronal structures (Castro-Torres et al., 2014). Myeloperoxidase (MPO) is a heme protein, released by leukocytes, and plays a crucial role in inflammation and oxidative stress at the cellular level. Liu and co-workers (2005) demonstrated that pirfenidone decreased the level of MPO during AR. Haemoxygenase-1 (HO-1) expression progressively increases with acute allograft rejection severity and it is correlated with MPO activity (Bonnell et al., 2004). HO-1 is induced by oxidative stress and it plays a decisive role in the pathophysiology of oxidant injuries and may also have cytoprotective functions. Its self-regulatory protective function has been shown in several transplantation models (Sato et al., 2001; Ke et al., 2012). Platelet derived growth factor (PDGF) plays a central role during the pathogenesis of fibrosis and chronic reaction in lungs (Kallio et al., 1999; Oyaizu et al., 2003; Ingram et al., 2004; Jaramillo et al., 2005) and can be influenced by oxidative stress parameters (Seidel et al., 2010).

Zhou and co-workers (2005) showed synergistic effects of pirfenidone in combination with a mammalian target of rapamycin (mTOR)-inhibitor in protecting against the development of allograft lesions. The immunosuppressive and antiproliferative properties of mTOR-inhibitors have already been shown in several *in vitro* (Nashan et al., 2002; Azzola et al., 2004) and *in vivo* (Schuler et al., 1997; Salminen et al., 2000) studies. However, only the co-application of the mTOR-inhibitor everolimus and the calcineurin-inhibitor cyclosporine (Hausen et al., 2000) or the PDGF-inhibitor imatinib (von Süsskind-Schwendi et al., 2013a), prevented allograft rejection.

The aim of our study was to investigate the efficacy of pirfenidone alone and in combination with an mTOR-inhibitor to reduce CR after experimental LTx by diminishing oxidative stress in the long term follow up.

Materials and methods

Experimental lung transplantation

Specific pathogen-free inbred male Fisher F344 (RT1lvl) and Wystar Kyoto WKY (RT1l) rats used in this study were obtained from Charles River (Harlan-Winkelmann, Borchen, Germany; 200±30 g). Orthotopic transplantations of left lung allografts (F344-to-WKY) were performed as described earlier (Hirt et al., 1999; von Suesskind-Schwendi et al., 2012). Briefly, donor lungs (F344) were dissected from ventilated living donors in deep anesthesia, flushed with cold Euro-Collins solution, and with 1-hour ischemia implanted orthotopically into recipients (WKY). The general health status of the recipients was assessed by daily weight measurement and intermittent observation of grooming behavior and feces. All animals received humane care in compliance with the Principles of Laboratory Animal Care formulated by the European Union Guide for the Care and Use of Laboratory Animals (publication No. 86/609/EWG). Approval was granted by the institutional ethical committee at the University of Regensburg.

Experimental designs

Four study groups were transplanted and treated according to Table 1. 16 transplantations in each group were studied: group (1) F344 (donor) to WKY (recipient) rats (untreated allografts), group (2) F344 to pirfenidone-fed WKY rats (pirfenidone-treated allografts), group (3): F344 to everolimus treated WKY rats (everolimus-treated allografts), and group (4): F344 to pirfenidone-fed and everolimus treated WKY rats (combined-treated allografts). Pirfenidone (InterMune, USA), 0.85% in chow, was started 3 days before transplantation. The pirfenidone dose (600 mg/kg bw) was chosen on the basis of prevention of interstitial fibrosis and allograft injury in other animal models in previous studies (Dosanjh et al., 2002). Dose of everolimus (Novartis Pharma, Basel, Switzerland) (2.5 mg/kg body weight, intragastral) was based on previous studies with this rat model (von Suesskind-Schwendi et al., 2013a). Microemulsion formulation of everolimus for oral administration was applicated daily in a single dose from postoperative day (POD) 7 throughout the experiment.

Animals were sacrificed on POD 20 (early, inflammatory phase of allograft rejection (acute rejection, AR)) and on POD 60 (late, fibroproliferative

Table 1. Study groups.

#	drug	Dosage (mg/kg bw per day)	Time of application (begin / end)
1	No	No	No
2	Pirfenidone	600 (in chow)[b]	POD -3 / POD 20/60
3	Everolimus	2.5 (intragastral)[c]	POD 7[a] / POD 20/60
4	Pirfenidone + Everolimus	Dito groups 2 and 3	Dito groups 2 and 3

[a], reasons for delayed application (Hirt et al., 1999; von Suesskind-Schwendi et al. 2013a): AR developed within 7 days after lung transplantation (LTX), risk of wound healing disorders, poor tolerance of the drug early after LTX. [b], according to Dosanjh 2007; [c], according to von Suesskind-Schwendi et al., 2013b. Bw, body weight; POD, postoperative day.

phase of allograft rejection (chronic rejection, CR)) (n=8 at each time point) and lungs (transplanted left lung, allograft; non-transplanted right lung, reference) were removed as described earlier (von Suesskind-Schwendi et al., 2013b).

Determination of pirfenidone in plasma

Heparinized blood samples were collected on POD -4, 9, 20 and 60 (at 11:00 am) from the tail vein, centrifuged and plasma was stored at -80°C until further processing. Plasma concentration of Pirfenidone was measured using High Performance Liquid Chromatography (HPLC) as described by Giri and co-workers (2002).

Histology

Acute rejection (AR) and chronic rejection (CR) was assessed in allografts and non-transplanted right lungs that were surgically removed, fixed in 10% buffered formalin, embedded in paraffin, sectioned into 5 μm thick sections and stained with hematoxylin-eosin (HE) (mononuclear infiltrations) and Sirius Red/Elastica-van Gieson (collagen type I and elastic fibers). Acute allograft rejection was graded according to the actual working formulation of The International Society for Heart and Lung Transplantation (ISHLT) (Stewart et al., 2007; von Suesskind-Schwendi et al., 2012). Briefly, acute vascular rejection was graded into A0-A4 depending on the extent of perivascular and interstitial mononuclear cell infiltrates. The degree of acute airway inflammation was scored from B0-B2R according to the extent and intensity of lymphocytic bronchiolitis. Chronic airway and chronic vascular rejection was quantified by the assessment of chronic altered bronchioles and small/medium-sized vessels. The degradation of the bronchioles was classified as none (no chronic alterations; C0), mild (first signs of granulation tissue into the small bronchioles; C1R), and severe (pronounced fibrotic degeneration; C2R) (von Suesskind-Schwendi et al., 2012, 2013b). In this context, severe chronic airway rejection (C2R/BO) was defined as an excessive proliferation of granulation tissue either within the airway wall (constructive bronchiolitis) or within its lumen (granulation tissue obliterates the lumen), or both. The same scoring system was used for small and medium-sized vessels (no chronic alterations; D0), mild degenerations (obstruction of small vessels with first signs of fibrotic degeneration; D1R) and severe degenerations (vasculopathy including distinct fibrotic degeneration of small and medium sized vessels; D2R). The percentage of all affected bronchioles (C) or vessels (D) relative to the total amount of structures per tissue section, was respectively used to quantify the degree of chronic airway and chronic vascular rejection (von Suesskind-Schwendi et al., 2013b). To evaluate the interstitial fibrotic damage of the section, we included an evaluation of the histological samples by a modified Ashcroft-scale (Hübner et al., 2008) (Table 2).

Immunohistopathology

The expression of myeloperoxidase (MPO), haemoxygenase-1 (HO-1) and platelet derived growth factor receptor alpha (PDGFRa) was assessed by immunohistochemistry using rabbit anti-human primary antibodies (MPO: DAKO, A0398, diluted 1:3000; PDGFR-a: Santa Cruz (c-20) sc338, diluted 1:1000; HO-1: Abcam, ab85309, diluted 1:1200). After deparaffinisation, tissue sections were heated for 20 min in 1x Target Retrieval Solution (Dako; S 2369) and treated with hydrogen peroxide to quench nonspecific peroxidases. Thereafter tissue sections were incubated in 10% normal rabbit serum for 30 min at room temperature to block non-specific binding sites. After rinsing with PBS, the sections were incubated with primary antibodies (rabbit anti-human MPO (DAKO, A0398, diluted 1:3000); PDGFR-a (Santa Cruz, c-20, sc338, diluted 1:1000); HO-1 (Abcam, ab85309, diluted 1:1200)) overnight at 4°C. After rinsing, sections were incubated first with biotinylated secondary goat anti-rabbit antibody (Vector BA-1000, diluted 1:300) for 1 hour at room temperature and then with streptavidin horseradish peroxidase conjugate (Vectastain, Vector Laboratories, Inc. Burlingame, USA, ABC kit, PK-6100). HistoGreen (Linaris-Biologische Produkte, Wertheim-Bettingen, Germany) was used as a specific

Table 2. Histological characterization of the modified Ashcroft scale (Hübner et al. ,2008).

Grade of Fibrosis	Characterization of the Modified Scale
0	Alveolar septa: no fibrotic alveolar walls Lung structure: Normal lung
1	Alveolar septa: Isolated fibrotic Lung structure: Alveoli partly enlarged and rarefied, but no fibrotic masses present
2	Alveolar septa: Clearly fibrotic changes with knot-like formation, not connected to each other Lung structure: Alveoli partly enlarged no fibrotic masses
3	Alveolar septa: Contiguous fibrotic walls Lung structure: Alveoli partly enlarged and no fibrotic masses
4	Alveolar septa: Variable Lung structure: Single fibrotic masses (≤10%of microscopic field)
5	Alveolar septa: Variable Lung structure: Confluent fibrotic masses (>10%and ≤50%of microscopic field). Lung structure severely damaged but still preserved
6	Alveolar septa: Variable, mostly not existent Lung structure: Large contiguous fibrotic masses (>50%of microscopic field). Lung architecture mostly not preserved
7	Alveolar septa: Non-existent Lung structure: Alveoli nearly obliterated with fibrous masses
8	Alveolar septa: Non-existent Lung structure: Microscopic field with complete obliteration with fibrotic masses

substrate chromogen (Thomas and Lemmer, 2005). Normal rabbit immunoglobulin G (Santa Cruz Biotechnology) was used as an isotype control. The amount of MPO-, HO-1- and PDGFR-a-positive cells were counted in a blinded fashion by 2 independent operators using 5 randomly selected microscopic high-power fields (400x) per graft.

Evaluation of iron

To assess the deposition of iron in the lungs, Prussian blue staining was used (Accustain HT20; Sigma Aldrich, Germany). Paraffin sections were stained according to manufacturer´s instructions. Prussian blue reaction involves the treatment of sections with acid solution of ferrocyanides. Any ferric ion (+3) present in the tissue combines with the ferrocyanide and results in the formation of a bright blue pigment (nuclei are red). The micrographs were observed by a microscope (Olympus BX 41, Germany) at 200x magnification. The images were then captured with a high-resolution 16 bit camera (Olympus color view soft imaging system) along with imaging software (ImageJ) to measure the gray value in the blue image channel.

Collagen measurement

Lung collagen (hydroxyproline) content was detected by a multiplex-enzyme-linked immunosorbent assay (ELISA) system (BlueGene; Rat Hydroxyproline Elisa kit). Briefly, frozen lung tissue was homogenized using Tissue Lyser LT (Quiagen, Valencia, CA), and hydrolysed with 6 M hydrochloric acid. Hydroxyproline content was determined according to the manufacturer´s instructions. The total amount of collagen in each sample was calculated, assuming that lung collagen contains 12.2% w/w hydroxyproline (Laurent et al., 1981), and expressed as μg collagen per mg lung tissue (Mutsaers et al., 1998).

Data requisition and analysis

Histological scoring was performed by three independent investigators in a blinded fashion. Data were expressed as means±standard error of the means (SEM). The Kruskal-Wallis test was used to compare all study groups on POD 20 and POD 60. A Wilcoxon-Mann-Whitney-U-test was used as a non-parametric statistical hypothesis test for assessing whether one study group tends to have improved during therapy compared to the individual study groups. Statistical package SPSS 18.0 (SPSS, Chicago, IL, USA) was used for statistical analysis. A P value ≤0.05 was considered statistically significant.

Results

Survival and general health

All successfully transplanted rats showed good general conditions (normal social and grooming behaviour, acceptable feed consumption, inconspicuous defecation). Drugs were well tolerated. During study period, mean plasma levels of pirfenidone (1.1±0.3 μg/ml) and everolimus (19.3±3.1 μg/l) remained unchanged. The plasma level of pirfenidone corresponds to the data of Mirkovic and co-workers (2002).

As shown in Figure 1, diet change including Pirfenidone did not affect body weight. Independent of drug treatment, early after LTX feed consumption was restricted (data not shown) and resulted in a significant decrease in mean body weight (8.4±0.4%, p≤0.05). Rats from groups 1 and 2 regained their initial body weight within 10.6±0.8 days and 14.4±0.9 days, respectively. Afterwards, body weight increased significantly over time (p≤0.001). Application of everolimus on POD 7 (groups 3 and 4) caused a mild secondary weight loss (1.8±0.3% and 3.1±1%, respectively). Recovery of secondary weight loss took 5.3±0.5 days and more than

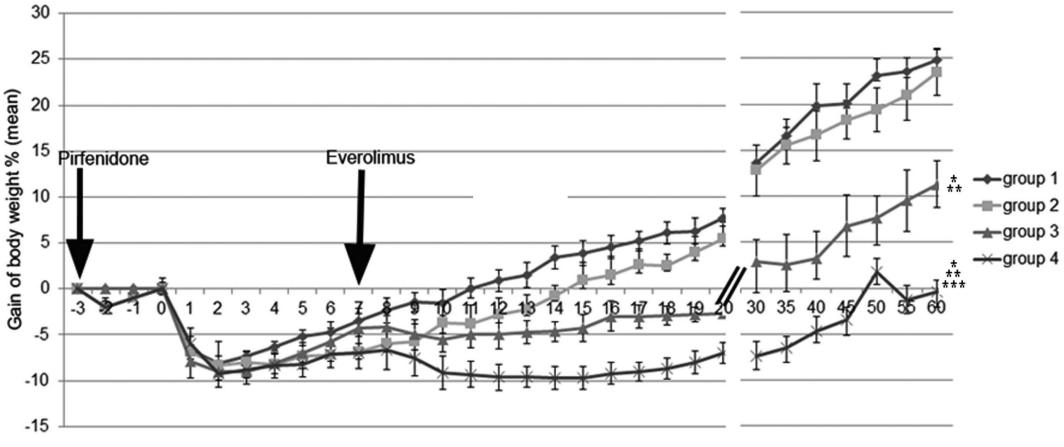

Fig. 1. Demonstrates the gain of body weight (mean±SEM) of group 1 (control), group 2 (pirfenidone), group 3 (everolimus) and group 4 (pirfenidone with everolimus). There is no significant difference between group 1 and 2. After treatment with everolimus, animals of group 3 and 4 showed a secondary weight loss and thereafter a significantly less gain of body weight compared to group 1 (*, p<0,05) and 2 (**, p<0,05). Gain of body weight of group 4 was significantly reduced compared to group 3 (***, p<0,05).

20 days, respectively. Weight gain of everolimus treated animals was significantly reduced compared to groups 1 and 2 ($p \leq 0.05$).

Effect of pirfenidone in the early stage after transplantation (POD 20)

Table 3 summarizes the effects of pirfenidone in the early stage after transplantation.

Acute allograft rejection

In the control group (group 1), alloimmune activation peaked on POD 20 (Suesskind-Schwendi et al., 2012). Representative micrographs from allografts of all study groups are shown in Fig. 2. Severe acute vascular (ISHLT-A3-4) and airway rejection ISHLT-B1R-2R) in addition to a prominent alveolar pneumocyte damage and endothelialitis dominated the tissue sections of all study groups (Fig. 2A-D). Only the combination therapy (group 4) demonstrated a slight improvement of acute cellular rejection (Table 3, not significant; Fig. 2D).

In addition to the ISHLT-classification, the inflammatory infiltration of the alveolar septa and the interstitium was reduced for some allografts treated with pirfenidone (group 2, 3/8 allografts; group 4, 4/8 allografts; Fig. 2B,D) compared to group 1 (8/8 allografts; Fig. 2A) and 3 (8/8 allografts; Fig. 2C). Right lungs were inconspicuous.

Oxidative stress on POD 20

This study analyzed the effect of drugs on different stress parameters on POD 20 such as expression of MPO (Liu et al., 2005), HO-1 (Bonnell et al., 2004) and

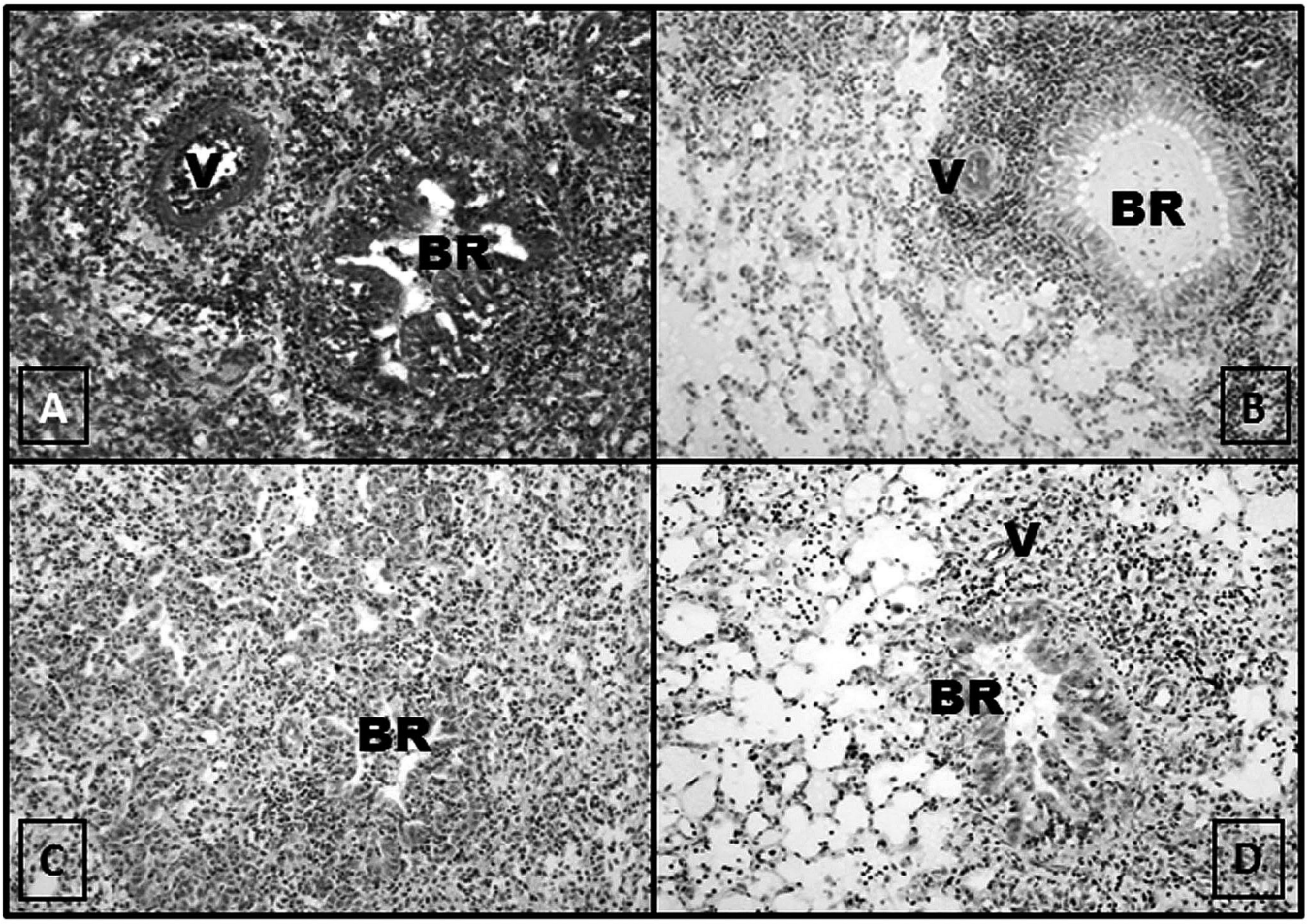

Fig. 2. Acute allograft rejection on POD 20. Histological evaluation of lung allografts. **A.** Representative lung allograft from non-treated rats (group 1). **B.** Pirfenidone treated rats (group 2). **C.** Everolimus treated rats (group 3). **D.** The combination group (group 4). **A and C.** Severe acute vascular rejection (ISHLT-A4) in combination with a high grade small airway inflammation. Mononuclear infiltrates are surrounding small vessels. Terminal bronchioles show evidence of epithelial damage in combination with a marked intra-epithelial lymphocytic infiltration., Alveolarsepta are highly infiltrated with mononuclear cells. **B and D.** Small vessels and bronchioles are cuffed by a mononuclear cell infiltrate. Sub-epithelial structures are less involved (ISHLT-A3/B1R). In these allografts, alveolar septa are infiltrated only sporadically with mononuclear cells. HE-staining, x 10

PDGFR-a (Ingram et al., 2004) (Table 3, Fig. 3). The expression of these stress parameters in right lungs was very low. Allogeneic transplantation without treatment (group 1) resulted in a significant increase in the amount of MPO-positive cells (factor of 4.2±0.9; p=0.012). While pirfenidone alone did not affect MPO expression, allografts from everolimus treated animals showed highest accumulation of MPO (group 3, p= 0.043; group 4; p= 0.001). Representative micrographs were presented in Figure 3A,B. The expression of HO-1 protein was significantly increased in highly rejected allografts from groups 1 (p=0.008) (Fig. 3C) and 2 (p=0.008). HO-1 staining was mainly localized in mononuclear cells and alveolar macrophages. Only a few bronchiolar epithelial cells appeared positive, whereas endothelial cells and type I pneumocytes revealed no HO-1 expression. Instead, everolimus treatment significantly reduced the number of HO-1-positive cells in the allografts from groups 3 (p=0.036) and 4 (p=0.08) (Fig. 3D). In contrast, in all study groups, the expression of PDGFR-a and the deposition of iron was very low (Table 3) and remained unchanged over time (data not shown).

Chronic allograft rejection on POD 20

Table 3 also included data on the early appearance of chronic bronchiolar rejection (ISHLT-C) and chronic vascular rejection (ISHLT-D). LTx without treatment caused degradation of about 50% of small vessels within 20 days after transplantation, while only 14% of the bronchioles showed moderate and severe fibrotic alterations. Independent of treatment strategy, the development of early signs of chronic airway rejection remained unchanged. In contrast, monotherapy with pirfenidone (group 2) or everolimus (group 3) tended to reduce the proportion of vessels with fibrotic alterations (not significant). A significant effect was documented for allografts from group 4. The most severe degree of chronic vascular degeneration (ISHLT-D2R) was more pronounced in groups 1 and 3 than in groups 2 and 4 (Table 3). Collagen measurement on POD 20 showed no difference between the groups.

Effect of pirfenidone in the long term follow up (POD 60)

Table 4 summarizes the effect of pirfenidone in the long term follow up. Representative micrographs of histologic alterations are present in Fig. 4.

Chronic allograft rejection (POD 60)

Up to day 60, histology of native, non-transplanted right lungs remained unchanged. In contrast, allogeneic transplanted left lungs developed high grade of chronic

Table 3. Effect of pirfenidone in the early stage after transplantation (POD 20).

	group 1 untreated	group 2 PIR	group 3 EVE	group 4 PIR/EVE	Right lungs
Acute allograft rejection					
ISHLT-A					
mean (SEM)	4.0 (0.0)	3.9 (0.1)	3.8 (0.1)	3.5 (0.2)	0.0
A0/A1/A2/A3/A4 (n)	0/0/0/0/8	0/0/0/1/7	0/0/0/3/5	0/0/0/5/3	32/0/0/0/0
ISHLT-B					
mean (SEM)	2.0 (0.0)	2.0 (0.0)	2.0 (0.0)	1.8 (0.2)	0.0
B0/B1R/B2R (n)	0/0/8	0/0/8	0/0/8	0/2/6	32/0/0
Oxidative Stress					
MPO[a]	14 (1) #	13 (2)	31 (3) #;§	38 (1) #;§	3 (2)
HO-1[a]	17 (3) #	19 (5) #	1 (2) §	2 (1) §	2 (1)
PDGFR-a[a]	6 (2)	4 (3)	3 (1)	4 (1)	6 (2)
Fe^{3+b}	223 (188)	384 (112)	512 (123)	319 (99)	291 (78)
Chronic allograft rejection					
ISHLT-C[c]	14	1	26	14	0
C0/C1R/C2R[d]	86/6/8	99/1/0	74/18/8	86/12/2	100/0/0
ISHLT-D[e]	50	23	15	15 §	0
D0/D1R/D2R[f]	50/32/18	77/21/2	85/4/11	85/13/2	100/0/0
Interstitial fibrosis[g]	0	0	0	0	0
Collagen[h]	180 (14)	90 (9)	n.d.	170 (29)	50 (15)

[a], number of positive cells per high power field (mean and SEM); [b], measured as grey value in the blue image channel (mean and SEM) [c], % of chronic affected bronchioles (C1R+C2R); [d], distribution of degradation classification of chronic affected bronchioles (% of all bronchioles); [e], % of chronic affected vessels (D1R+D2R); [f], distribution of degradation classification of chronic affected vessels (% of all vessels); [g], grade of interstitial fibrosis (Ashcroft scale 0-8) (mean and SEM); [h], μg collagen per mg lung tissue (mean and SEM). N.d., not detected. PIR, pirfenidone treated animals; EVE, everolimus treated animals; PIR/EVE, combination therapy; Statistics: #, significant vs. right lungs ($p \leq 0.05$); §, significant vs group 1 ($p \leq 0.05$);

alterations of bronchioles and vessels (group 1). The majority of bronchioles and vessels were identified with severe chronic degenerations (ISHLT-C2R, C2R, 75±16%; ISHLT-D2R, 76±9.8%), including highest content of peribronchiolar/intraluminal and perivascular/intravascular collagen depositions and a high grade of interstitial fibrosis (Table 4, Fig. 4A). Monotherapy with pirfenidone (group 2) and everolimus (group 3) did not improve the development of chronic vascular rejection (ISHLT-D) and the grade of interstitial fibrosis, but significantly reduced chronic bronchiolar alterations (ISHLT-C, group 2, 66±14%, p=0.05; group 3, 68±12%,

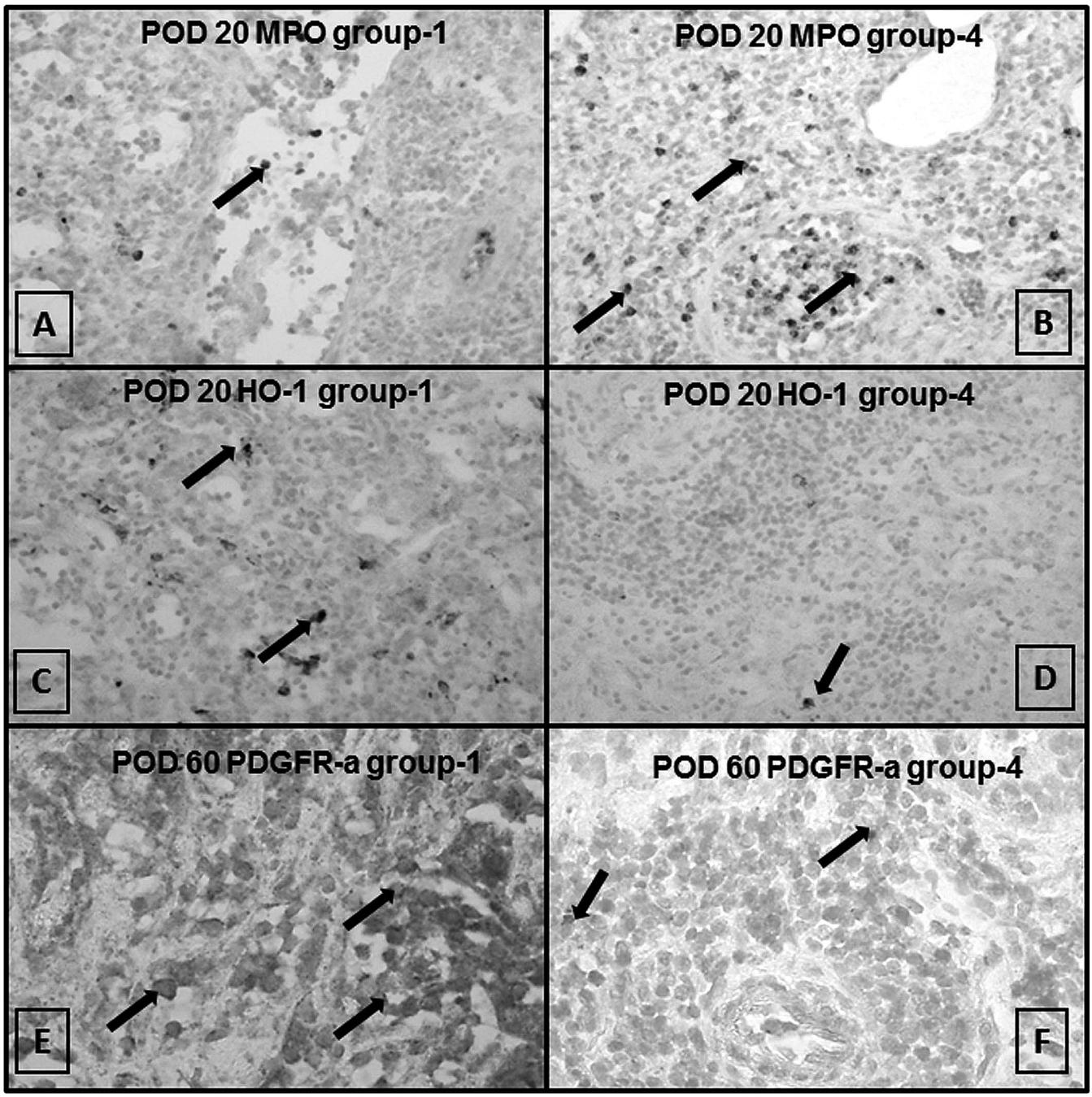

Fig. 3. Immunohistochemical staining of MPO (HistoGreen), HO-1 (HistoGreen) and PDGFR-a (HistoGreen) in lung allografts of group 1 **(A, C and E)** and group 4 **(B, D and F)**. The arrows point to MPO-, HO-1- and PDGFR-a-positive cells. A-D, x 20; E, F, x 40

p=0.04), and the content of collagen (group 2) (Table 4). Particularly noticeable was the proportion of non-affected bronchioles that increased by a factor of 2 and of bronchioles with severe alterations (C2R) that decreased by a factor of 1.5 to 3. The content of collagen from everolimus-treated allografts (group 3) was not analysed due to less lung tissue.

The most promising long-term effect was documented for animals treated with a combination of pirfenidone and everolimus (group 4). The allografts from group 4 presented a significant reduction of fibrotic bronchioles (ISHLT-C, 40±12.8%, p=0.001), small vessels (ISHLT-D, 14±4.4%, p=0.001), and interstitial fibrosis (2.3±0.7, p=0.029) (Fig. 4D). Both the proportion of non-affected vessels (ISHLT-D0, 86±11%, p=0.001) and bronchioles (ISHLT-C0, 55±12.1%, p=0.012) were significantly higher compared to allografts from non-treated rats. The content of collagen remained unchanged compared to group 2. A comparison with everolimus-treatment (group 3) failed (see above).

Against the background that chronic rejection was progressed in the allografts from group 1, the chronic inflammation faded. A reduction in the degree of chronic rejection was accompanied with more infiltration of mononuclear cells on POD 60 (Fig. 4B,D).

Oxidative stress in the long term follow up

Chronic oxidative stress may be implicated in the development and progression of BO (Madill et al., 2009). In the long-term follow-up after LTx, while the

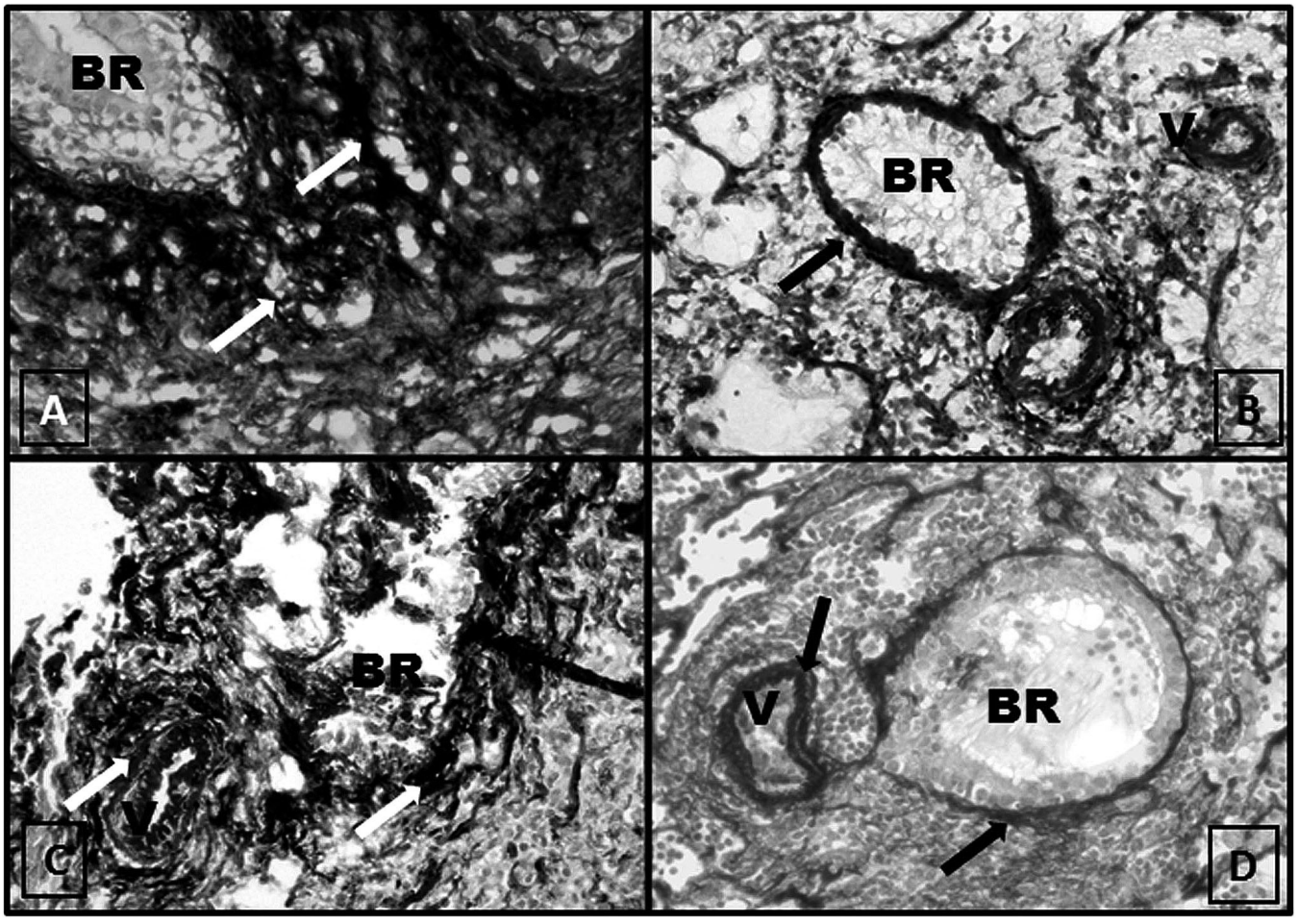

Fig. 4. Chronic allograft rejection on POD 60. Histological evaluation of lung allografts (Sirius Red-staining). **A.** Representative lung allograft from non-treated rats of group 1. **B.** pirfenidone treated rats. **C.** Everolimus treated rats. **D.** The combination group (pirfenidone and everolimus). **A.** Severe chronic rejection (ISHLT-C2R/D2R) dominates the histological section on POD 60 in the allografts of the non-treated rats. A reduction of collagen I fibers can be observed in group 2 **(B)** (ISHLT-C1R/D1R), group 3 **(C)** (ISHLT-C1R-C2R/D2R) and group 4 **(D)** (ISHLT-C0/D0). Arrows show the formation of collagen fibers in all sections. x 10

Table 4. Effect of pirfenidone in the long-term follow-up (POD 60).

	group 1 untreated	group 2 PIR	group 3 EVE	group 4 PIR/EVE	Right lungs
Chronic allograft rejection					
ISHLT-C[a]	90	66 §	68 §	40§	0
C0/C1R/C2R[b]	10/5/75	34/39/27	32/14/54	55/22/23	100/0/0
ISHLT-D[c]	85	76	66	14 §	0
D0/D1R/D2R[d]	15/9/76	24/35/41	34/0/66	86/5/9	100/0/0
Interstitial fibrosis[e]	7 (2) #	6 (1) #	6 (2) #	2 (1) #;§	0
Collagen[f]	680 (27) #	360 (75) #;§	n.d.	320(43) #;§	30 (14)
Oxidative Stress					
MPO[g]	8 (1)	9 (1)	8 (1)	10 (1)	6 (1)
HO-1[g]	8 (2) #	17 (1) #;§	2 (1)	17 (2) #;§	2 (2)
PDGFR-a[g]	36 (5) #	5 (1) §	2 (1) §	2 (1) §	8 (2)
Fe^{3+h}	4336 (868) #	874 (354) §	1263 (317) §	679 (278) §	381 (122)

[a], % of chronic affected bronchioles (C1R+C2R); [b], distribution of degradation classification of chronic affected bronchioles (% of all bronchioles); [c], % of chronic affected vessels (D1R+D2R); [d], distribution of degradation classification of chronic affected vessels (% of all vessels); [e], grade of interstitial fibrosis (Ashcroft scale 0-8) (mean and SEM); [f], μg collagen per mg lung tissue (mean and SEM); [g], number of positive cells per high power field (mean and SEM); [h], measured as grey value in the blue image channel (mean and SEM). N.d., not detected; PIR, pirfenidone treated animals; EVE, everolimus treated animals; PIR/EVE, combination therapy;Statistics: #, significant vs. right lungs ($p \leq 0.05$); §, significant vs group 1 ($p \leq 0.05$).

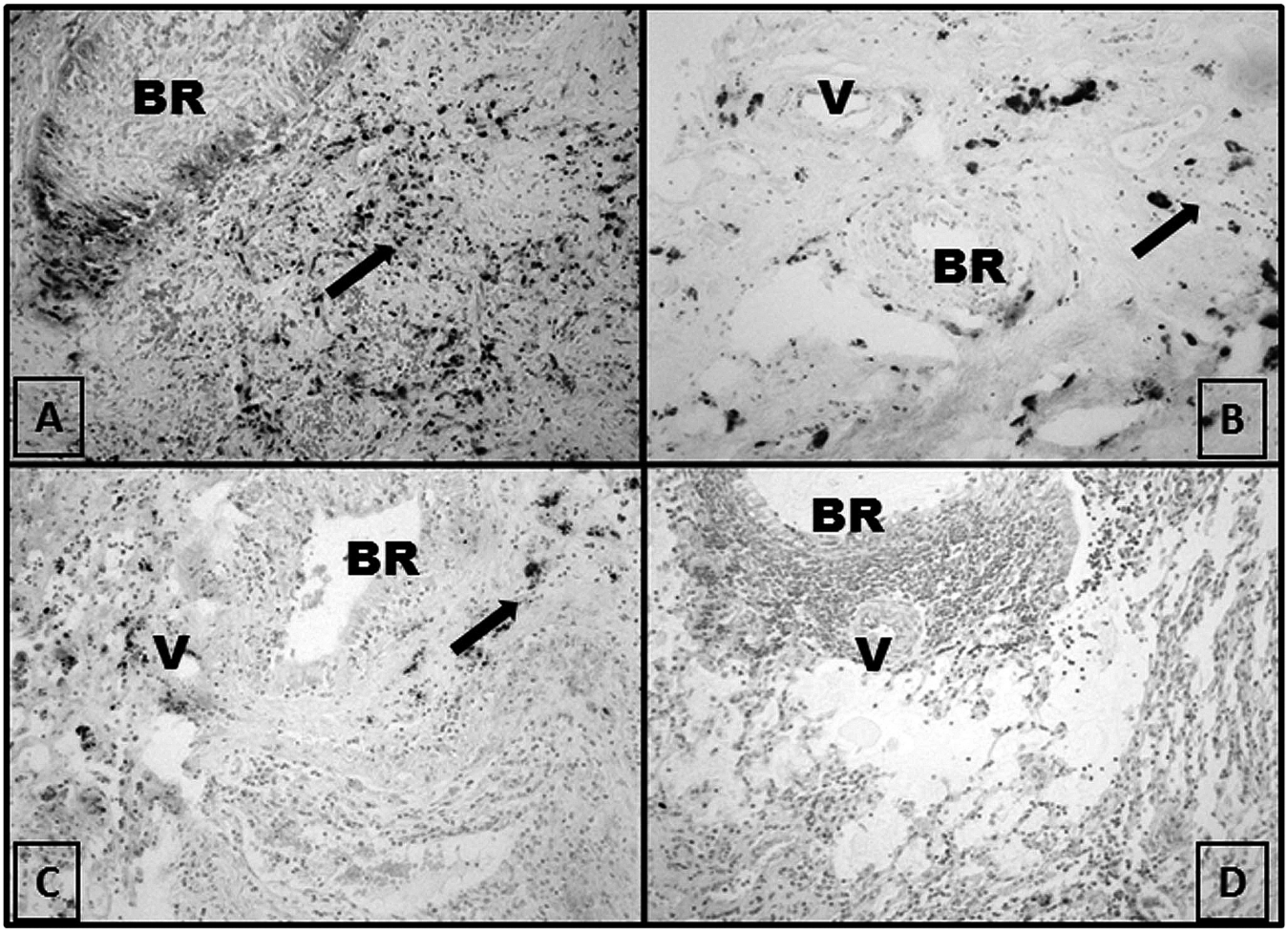

Fig. 5. Histological evaluation of lung allografts on POD 60 (iron-staining). **A.** Representative lung allograft from non-treated rats (group 1). **B.** Pirfenidone treated rats. **C.** Everolimus treated rats. **D.** The combination group (pirfenidone and everolimus). The stored iron presents itself as a dark (blue) complex. Arrows indicate the iron complexes in the different groups. While a strong iron exposure was observed in the non-treated control group **(A)**, a low iron storage was detected in group 4 **(D)**. x 10

recruitment of MPO-positive cells was not relevant to verify chronic oxidative stress, significant differences in the expression of HO-1 and PDGFR-a as well as the incorporation of iron proved the relevance of these parameters to disclose the effect of different treatment strategies on the development of chronic alterations. The density of HO-1-positive cells was significantly increased in the allografts from group 1 compared to respective right lungs (p=0.016). A further accumulation of HO-1-positive cells was documented in allografts from rats treated with pirfenidone (group 2, p=0.016; group 4, p=0.016; compared to group 1). Instead, monotherapy with everolimus suppressed the expression of HO-1 (comparable with the density in right lungs). The combination of everolimus with pirfenidone (group 4) did not change the expression of HO-1 compared to group 2. Nevertheless, over time, the number of HO-1-positive cells per microscopic field decreased in group 1, remained high in group 2, remained low in group 3, and increased significantly in group 4.

The expression of PDGFR-a was significantly increased in allografts from group 1 (p=0.048) (Fig. 3E). In these lungs, PDGFR-a was mainly localized in epithelial cells, metaplastic epithelial cells, fibroblast-like cells as well as in mononuclear cells. The expression of PDGFR-a was low in endothelial cells. All other treatment strategies significantly prevented the expression of PDGFR-a in the allografts (group 2, p=0.04; group 3, p=0.04; group 4, p=0.028). There was no difference between the study groups and the respective non-transplanted right lungs. Nevertheless, over time, the expression of PDGFR-a only increased in group 1, while the expression remained suppressed in the study groups 2-4.

Pirfenidone-induced regulation of the iron deposition in the lungs might be an indicator for reduced oxidative stress (Turi et al., 2004; Liu et al., 2005). Sections from non-transplanted right lungs displayed less iron staining. By contrast, highest positive staining was observed in allografts from untreated animals (p=0.002) (group 1, Fig. 5A), whereas the amount of stainable iron was significantly reduced in allografts from all other study groups (group 2, p=0.03; group 3, p=0.05; group 4, p=0.01). Over time, the degree of iron deposition increased significantly in allografts from all animals. However, the increase was less pronounced in groups 2 to 4 (xfold increase over time, group 1, 11±2.0; group 2, 2±1.0; group 3, 3±1.5; group 4, 2±0.5).

Discussion

The present study showed that early application of pirfenidone inhibited the progression of chronic allograft rejection after experimental LTx. While the anti-inflammatory properties of pirfenidone were restricted to reduced inflammatory infiltrations of the alveolar septa and the interstitium, pirfenidone suppressed early fibrotic degenerations and prolonged the cytoprotective function of HO-1 to reduce oxidative stress injury in the allograft. Pirfenidone alone significantly reduced chronic airway rejection, interstitial fibrosis, content of collagen, expression of PDGFR-a and the deposition of iron. The additional application of everolimus amplified the anti-fibrotic properties of pirfenidone resulting in a significant decrease in the extent of BO, vasculopathy and interstitial fibrosis in the allografts.

BO and vasculopathy are caused by inflammatory and fibroproliferative reactions (Stewart et al., 2007). Underlying mechanisms are frequently unresponsive to augmentation of immunosuppression (Behr et al., 2000; Glanville et al., 2015) and may be of relevance for the evolving process (Behr et al., 2000). Behr and co-workers (2000) demonstrated that neutrophilia in the lower respiratory tract, which is generally not influenced by immunosuppressants, was a prominent feature in Bronchiolitis obliterans syndrome, the clinical correlate of BO. The role of oxidant injury and increased neutrophil activity in the genesis of AR and bronchiolitis obliterans has recently been appreciated in animal models (Siraishi et al., 1997; Riise et al., 1998; Bonell et al., 2004) and humans (Lu et al., 2002). Similar results were shown in our rat model. Neutrophil influx increased during early acute cellular rejection as verified by high numbers of MPO-positive cells. MPO is expressed in neutrophils and catalyses the reaction between hydrogen peroxide and chloride to form a highly reactive species, hypochlorus acid. Therefore, MPO is an indirect marker for oxidative stress in lung allografts (Bonnell et al., 2004; Liu et al., 2005) and a stimulus for HO-1 (Lu et al., 2002). HO-1 has cytoprotective functions whereby HO-1 is important against oxidative stress injury (Le et al., 1999; Sato et al., 2001; Ke et al., 2012).

In this study, pirfenidone alone or in combination with everolimus did not inhibit oxidative stress and the development of acute cellular rejection in the early time after transplantation. These results seem to be in contrast to the results of Liu and co-workers (2005), who described a significant reduction of MPO-positive cells in an acute LTx rat model. Reasons for opposing results might be usage of different animal models or problems in installation of stable pirfenidone blood-levels within the first days after transplantation. Since pirfenidone was given by feed and our rats showed a restrained feed intake during the first three days after surgery, it cannot be excluded that the ultimate dosage was achieved too late to inhibit oxidative processes. It was already shown by Zhou and co-workers (2005) that an early therapeutic blood level of pirfenidone might be decisive for the success of therapy. Therefore, further studies focusing on optimal drug uptake during the first days after transplantation (for example application per gavage during the first four days after transplantation) might improve the outcome after LTx. Nevertheless, it should be emphasized that pirfenidone treatment decreased the extent of inflammatory infiltrations within the alveolar septa and the interstitium. However, this distinctive feature was not included in the ISHLT classification. In

this context, it may be considered whether pirfenidone has more influence on the restrictive allograft syndrome (RAS). RAS is another form of chronic allograft rejection which takes place more in the interstitial area (Verleden et al., 2014) and can occur in addition to BO. Due to the fact that we can see bronchiolar, vascular and interstitial damage in our model, an evaluation of RAS might be possible.

In our model, the anti-oxidative properties of pirfenidone appeared on POD 60. Pirfenidone significantly reduced chronic airway rejection, interstitial fibrosis, content of collagen, expression of PDGFR-a and the deposition of iron. The additional application of everolimus amplified the anti-fibrotic properties of pirfenidone resulting in a significant decrease in the extent of fibrotic degeneration of the terminal bronchioles, vasculopathy and interstitial fibrosis in the allografts (see table 4), which can be considered as a reduction of BO and RAS.

Pirfenidone showed its anti-oxidative properties by maintaining HO-1 level. The cytoprotective and anti-proliferative properties of HO-1 in lung disease have already been reviewed by Constantin and co-workers (2012). In vascular smooth muscle cells it has been demonstrated that HO-1 products, CO and bilirubin, have been implicated to inhibit cell proliferation by promoting cell cycle arrest at G1/S phase and by attenuating cell migration effectively by inactivating platelet derived growth factor (PDGF) –receptor beta signaling (Cheng et al., 2012). The correlation between HO-1 and PDGF has also been demonstrated in an *in vitro* airway wall remodeling model (Seidel et al., 2010). It was shown that PDGF induced proliferation can be inhibited through a p38 MAPK dependent induction of HO-1. The effect of pirfenidone on the inhibition of PDGF-isoforms has already been confirmed by Gurujeyalashmi and co-workers (1999) in a bleomycin hamster model of lung fibrosis. We demonstrated that treatment with pirfenidone decreased PDGFR-a in rat allografts. Consequently, it can be speculated that pirfenidone might act via the inhibition of PDGF. Generally PDGF acts via the activation of MAPkinases. An inhibition of PDGF results in a decreased fibroblast proliferation which consequently reduces fibrotic degeneration in the long term course.

Moreover, it was described that pirfenidone inhibits the expression of collagen type I directly and indirectly by attenuating key TGF-β-induced signaling pathways in TGF-ß-stimulated human lung fibroblasts *in vitro* (Hisatomi et al., 2012; Conte et al., 2014) and in TGF-ß and PDGF-BB-stimulated renal tubular epithelial cells *in vitro* (Takakura et al., 2012).

However, more detailed studies on the mechanism of action of pirfenidone are needed. Novel studies in hepatic stellate cells (HSC) with a novel pyridone argent (Flurofenidone) demonstrated that the pyridone substances alter the balance between collagen synthesis and degradation *in vitro* and *in vivo* by the inhibition of MAPK signaling pathways in HSCs (Peng et al., 2013).

Especially the combination of pirfenidone and everolimus showed the best long-term results in terms of reducing chronic changes of the allografts after LTx. The mechanism of action of everolimus is described by the growth retardation by cell cycle arrest in G1-phase of the cell cycle (Grozinsky-Glasberg et al., 2010; Albanell et al., 2007). Strikingly, Yuge and co-workers (2015) recently showed that everolimus alone showed no effect on PDGF-pathways in human osteosarcoma cell lines MG63, while the phosphorylation of PDGF-R was significantly inhibited with everolimus in combination with a receptor-tyrosin-kinase-inhibitor (Nilotinib). Our results showed that even monotherapy with everolimus resulted in a reduction of the PDGFR-a. Anyway, only the combination of both substances presented a significant reduction of chronic bronchiolar and chronic vascular degeneration on POD 60.

The mechanism of action of pirfenidone, including the inhibition of oxidative stress, in combination with the anti-proliferative effect of the mTOR inhibitor everolimus seems to be a good way to reduce the progression of CR after LTx.

In conclusion, we suggest that oxidative stress plays a crucial role in the development of CR. In this study we demonstrated that pirfenidone reduced chronic graft failure via maintaining the cytoprotective enzyme HO-1. Additional therapy with everolimus could enhance the anti-fibrotic properties of pirfenidone. So we suggest that the combination therapy of pirfenidone and everolimus might be a promising therapeutic option after LTx.

Acknowledgements. The study was supported by a grant from InterMune, Brisbane, USA.

References

Albanell J., Dalmases A., Rovira A. and Rojo F. (2007). mTOR signalling in human cancer. Clin. Transl. Oncol. 9, 484-493.

Azzola A., Havryk A., Chhajed P., Hostettler K., Black J., Johnson P., Roth M., Glanville A. and Tamm M. (2004). Everolimus and mycophenolate mofetil are potent inhibitors of fibroblast proliferation after lung transplantation. Transplantation 27, 275-280.

Behr J., Maier K., Braun B., Schwaiblmair M. and Vogelmeier C. (2000). Evidence for oxidative stress in bronchiolitis obliterans syndrome after lung and heart-lung transplantation. The Munich Lung Transplant Group. Transplantation 15, 1856-1860.

Bonnell M.R., Visner G.A., Zander D.S., Mandalapu S., Kazemfar K., Spears L. and Beaver T.M. (2004). Heme-oxygenase-1 expression correlates with severity of acute cellular rejection in lung transplantation. J. Am. Coll. Surg. 198, 945-952.

Castro-Torres R.D., Chaparro-Huerta V., Flores-Soto M.E., Bañuelos-Pineda J., Camins A., Orozco-Suárez S.A., Armendáriz-Borunda J. and Beas-Zárate C. (2014). A single dose of pirfenidone attenuates neuronal loss and reduces lipid peroxidation after kainic acid-induced excitotoxicity in the pubescent rat hippocampus. J. Mol. Neurosci. 52, 193-201.

Cheng C., Haasdijk R.A., Tempel D., den Dekker W.K., Chrifi I.,

Blonden L.A., van de Kamp E.H., de Boer M., Bürgisser P.E., Noorderloos A., Rens J.A., ten Hagen T.L. and Duckers H.J. (2012). PDGF-induced migration of vascular smooth muscle cells is inhibited by heme oxygenase-1 via VEGFR2 upregulation and subsequent assembly of inactive VEGFR2/PDGFRβ heterodimers. Arterioscler. Thromb. Vasc. Biol. 32, 1289-1298.

Cheresh P., Kim S.J., Tulasiram S. and Kamp D.W. (2013). Oxidative stress and pulmonary fibrosis. Biochim. Biophys. Acta 1832, 1028-1040.

Constantin M., Choi A.J., Cloonan S.M. and Ryter S.W. (2012). Therapeutic potential of heme oxygenase-1/carbon monoxide in lung disease. Int. J. Hypertens. 2012, 859235.

Conte E., Gili E., Fagone E., Fruciano M., Iemmolo M. and Vancheri C. (2014). Effect of pirfenidone on proliferation, TGF-β-induced myofibroblast differentiation and fibrogenic activity of primary human lung fibroblasts. Eur. J. Pharm. Sci. 16, 13-19.

Dosanjh A., Ikonen T., Wan B. and Morris R.E. (2002). Pirfenidone: A novel anti-fibrotic agent and progressive chronic allograft rejection. Pulm. Pharmacol. Ther. 15, 433-437.

Dosanjh A. (2007). Pirfenidone: a novel potential therapeutic agent in the management of chronic allograft rejection. Transplant. Proc. 39, 2153-2156.

Gao F., Kinnula V.L., Myllärniemi M. and Oury T.D. (2008). Extracellular superoxide dismutase in pulmonary fibrosis. Antioxid. Redox Signal. 10, 343-354.

Giri S.N., Wang Q., Xie Y., Lango J., Morin D., Margolin S.B. and Buckpitt A.R. (2002).Pharmacokinetics and metabolism of a novel antifibrotic drug pirfenidone, in mice following intravenous administration. Biopharm. Drug Dispos. 23, 203-211.

Glanville A.R., Aboyoun C., Klepetko W., Reichenspurner H., Treede H., Verschuuren E.A., Boehler A., Benden C., Hopkins P. and Corris P.A.; for the European and Australian Investigators in Lung Transplantation (2015).Three-year results of an investigator-driven multicenter, international, randomized open-label de novo trial to prevent BOS after lung transplantation. J. Heart. Lung. Transplant. 34, 16-25.

Grozinsky-Glasberg S., Rubinfeld H., Nordenberg Y., Gorshtein A., Praiss M., Kendler E., Feinmesser R., Grossman A.B. and Shimon I. (2010). The rapamycin-derivative RAD001 (everolimus) inhibits cell viability and interacts with the Akt-mTOR-p70S6K pathway in human medullary thyroid carcinoma cells. Mol. Cell. Endocrinol. 5, 87-94.

Gurujeyalakshmi G., Hollinger M.A. and Giri S.N. (1999). Pirfenidone inhibits PDGF isoforms in bleomycin hamster model of lung fibrosis at the translational level. Am. J. Physiol. 276, 311-318.

Hausen B., Boeke K., Berry G.J., Christians U., Schüler W. and Morris R.E. (2000) Successful treatment of acute, ongoing rat lung allograft rejection with the novel immunosuppressant SDZ-RAD. Ann. Thorac Surg. 69, 904-909.

Hirt S.W., You X.M., Möller F., Boeke K., Starke M., Spranger U. and Wottge H.U. (1999) Development of obliterative bronchiolitis after allogeneic rat lung transplantation: implication of acute rejection and the time point of treatment. J. Heart Lung Transplant. 18, 542-548.

Hisatomi K., Mukae H., Sakamoto N., Ishimatsu Y., Kakugawa T., Hara S., Fujita H., Nakamichi S., Oku H., Urata Y., Kubota H., Nagata K. and Kohno S. (2012). Pirfenidone inhibits TGF-β1-induced over-expression of collagen type I and heat shock protein 47 in A549 cells. BMC Pulm. Med. 13, 12-24.

Hübner R.H., Gitter W., El Mokhtari N.E., Mathiak M., Both M., Bolte H., Freitag-Wolf S. and Bewig B. (2008). Standardized quantification of pulmonary fibrosis in histological samples. Biotechniques 44, 514-517.

Ingram J.L., Rice A.B., Geisenhoffer K., Madtes D.K. and Bonner J.C. (2004). IL-13 and IL-1beta promote lung fibroblast growth through coordinated up-regulation of PDGF-AA and PDGF-Ralpha. FASEB J. 18, 1132-1134.

Jaramillo A., Fernández F.G., Kuo E.Y., Trulock E.P., Patterson G.A. and Mohanakumar T. (2005). Immune mechanisms in the pathogenesis of bronchiolitis obliterans syndrome after lung transplantation. Pediatr. Transplant. 9, 84-93.

Ji X., Naito Y., Weng H., Ma X., Endo K., Kito N., Yanagawa N., Yu Y., Li J. and Iwai N. (2013). Renoprotective mechanisms of pirfenidone in hypertension-induced renal injury: through anti-fibrotic and anti-oxidative stress pathways. Biomed. Res. 34, 309-319.

Kallio E.A., Koskinen P.K., Aavik E., Buchdunger E. and Lemström K.B. (1999). Role of platelet-derived growth factor in obliterative bronchiolitis (chronic rejection) in the rat. Am. J. Respir. Crit. Care Med. 160, 1324-1332.

Ke B., Shen X.D., Ji H., Kamo N., Gao F., Freitas M.C., Busuttil R.W. and Kupiec-Weglinski J.W. (2012). HO-1-STAT3 axis in mouse liver ischemia/reperfusion injury: regulation of TLR4 innate responses through PI3K/PTEN signaling. J. Hepatol. 56, 359-366.

Laurent G.J., Cockerill P., McAnulty R.J. and Hastings J.R. (1981). A simplified method for quantitation of the relative amounts of type I and type III collagen in small tissue samples. Anal. Biochem. 113, 301-312.

Le W.D., Xie W.J. and Appel S.H. (1999). Protective role of heme oxygenase-1 in oxidative stress-induced neuronal injury. J. Neurosci. Res. 15, 652-658.

Liu H., Drew P., Cheng Y. and Visner G.A. (2005). Pirfenidone inhibits inflammatory responses and ameliorates allograft injury in a rat lung transplant model. J. Thorac. Cardiovasc. Surg. 130, 852-858.

Lu F., Zander D.S. and Visner G.A.(2002). Increased expression of heme oxygenase-1 in human lung transplantation. J. Heart Lung Transplant. 21, 1120-1126.

Madill J., Aghdassi E., Arendt B., Hartman-Craven B., Gutierrez C., Chow C.W. and Allard J (2009). University Health Network. Lung transplantation: does oxidative stress contribute to the development of bronchiolitis obliterans syndrome? Transplant. Rev. (Orlando). 23, 103-110.

Mallol J., Aguirre V. and Espinosa V. (2011). Increased oxidative stress in children with post infectious bronchiolitis obliterans. Allergol. Immunopathol. (Madr). 39, 253-258.

McKane B.W., Fernandez F., Narayanan K., Marshbank S., Margolin S.B., Jendrisak M and Mohanakumar T. (2004). Pirfenidone inhibits obliterative airway disease in a murine heterotopic tracheal transplant model. Transplantation 15;77, 664-669.

Mirkovic S., Seymour A.M., Fenning A., Strachan A., Margolin S.B., Taylor S.M. and Brown L. (2002). Attenuation of cardiac fibrosis by pirfenidone and amiloride in DOCA-salt hypertensive rats. Br. J. Pharmacol. 135, 961-968.

Mitani Y., Sato K., Muramoto Y., Karakawa T., Kitamado M., Iwanaga T., Nabeshima T., Maruyama K., Nakagawa K., Ishida K. and Sasamoto K. (2008). Superoxide scavenging activity of pirfenidone-iron complex. Biochem. Biophys. Res. Commun. 18, 19-23.

Mutsaers S.E., Foster M.L., Chambers R.C., Laurent G.J. and McAnulty R.J. (1998). Increased endothelin-1 and its localization during the development of bleomycin-induced pulmonary fibrosis in rats. Am J. Respir. Cell Mol. Biol. 18, 611-619.

Nashan B. (2002). Review of the proliferation inhibitor everolimus. Expert Opin. Investig. Drugs 11, 1845-1857.

Oyaizu T., Okada Y., Shoji W., Matsumura Y., Shimada K., Sado T., Sato M. and Kondo T. (2003). Reduction of recipient macrophages by gadolinium chloride prevents development of obliterative airway disease in a rat model of heterotopic tracheal transplantation. Transplantation 27, 1214-1220.

Peng Y., Yang H., Zhu T., Zhao M., Deng Y., Liu B., Shen H., Hu G., Wang Z. and Tao L. (2013). The antihepatic fibrotic effects of fluorofenidone via MAPK signalling pathways. Eur. J. Clin. Invest. 43, 358-368.

Ray P., Devaux Y., Stolz D.B., Yarlagadda M., Watkins S.C., Lu Y., Chen L., Yang X.F. and Ray A. (2003). Inducible expression of keratinocyte growth factor (KGF) in mice inhibits lung epithelial cell death induced by hyperoxia. Proc. Natl. Acad. Sci. USA 13, 6098-6103.

Riise G.C., Williams A., Kjellström C., Schersten H., Andersson B.A. and Kelly F.J. (1998). Bronchiolitis obliterans syndrome in lung transplant recipients is associated with increased neutrophil activity and decreased antioxidant status in the lung. Eur. Respir. J. 12, 82-88.

Salminen U.S., Maasilta P.K., Taskinen E.I., Alho H.S., Ikonen T.S. and Harjula A.L. (2000). Prevention of small airway obliteration in a swine heterotopic lung allograft model. J. Heart Lung Transplant. 19, 193-206.

Sato K., Balla J., Otterbein L., Smith R.N., Brouard S., Lin Y., Csizmadia E., Sevigny J., Robson S.C., Vercellotti G., Choi A.M., Bach F.H. and Soares M.P. (2001). Carbon monoxide generated by heme oxygenase-1 suppresses the rejection of mouse-to-rat cardiac transplants. J. Immunol. 15, 4185-4194.

Schuler W., Sedrani R., Cottens S., Häberlin B., Schulz M., Schuurman H.J., Zenke G., Zerwes H.G. and Schreier M.H. (1997) SDZ RAD, a new rapamycin derivative: pharmacological properties *in vitro* and *in vivo*. Transplantation 15, 36-42.

Scott A.I., Sharples L.D. and Stewart S. (2005). Bronchiolitis obliterans syndrome: risk factors and therapeutic strategies. Drugs 65, 761-771.

Seidel P., Goulet S., Hostettler K., Tamm M. and Roth M. (2010). DMF inhibits PDGF-BB induced airway smooth muscle cell proliferation through induction of heme-oxygenase-1. Respir Res. 20, 145.

Shiraishi T., Kuroiwa A., Shirakusa T., Kawahara K., Yoneda S., Kitano K., Okabayashi K. and Iwasaki A.(1997). Free radical-mediated tissue injury in acute lung allograft rejection and the effect of superoxide dismutase. Ann. Thorac. Surg. 64, 821-825.

Stewart S., Fishbein M.C., Snell G.I., Berry G.J., Boehler A., Burke M.M., Glanville A., Gould F.K., Magro C., Marboe C.C., McNeil K.D., Reed E.F., Reinsmoen N.L., Scott J.P., Studer S.M., Tazelaar H.D., Wallwork J.L., Westall G., Zamora M.R., Zeevi A. and Yousem S.A. (2007). Revision of the 1996 working formulation for the standardization of nomenclature in the diagnosis of lung rejection. J. Heart Lung Transplant. 26, 1229-1242.

Takakura K., Tahara A., Sanagi M., Itoh H. and Tomura Y. (2012). Antifibrotic effects of pirfenidone in rat proximal tubular epithelial cells. Ren. Fail. 34, 1309-1316.

Thomas M.A. and Lemmer B. (2005). HistoGreen: a new alternative to 3,3'-diaminobenzidine-tetrahydrochloride-dihydrate (DAB) as a peroxidase substrate in immunohistochemistry? Brain. Res. Brain. Res. Protoc. 14, 107-118.

Todd N.W., Luzina I.G. and Atamas S.P. (2012). Molecular and cellular mechanisms of pulmonary fibrosis. Fibrogenesis Tissue Repair 23, 11.

Turi J.L., Yang F., Garrick M.D., Piantadosi C.A. and Ghio A.J. (2004). The iron cycle and oxidative stress in the lung. Free Radic. Biol Med. 1, 850-857.

Verleden G.M., Raghu G., Meyer K.C., Glanville A.R. and Corris P. (2014). A new classification system for chronic lung allograft dysfunction. J. Heart Lung Transplant. 33, 127-133.

von Suesskind-Schwendi M., Ruemmele P., Schmid C., Hirt S.W. and Lehle K. (2012). Lung transplantation in the fischer 344-wistar kyoto strain combination is a relevant experimental model to study the development of bronchiolitis obliterans in the rat. Exp. Lung Res. 38, 111-123.

von Suesskind-Schwendi M., Brunner E., Hirt S.W., Diez C., Ruemmele P., Puehler T., Schmid C. and Lehle K. (2013a). Suppression of bronchiolitis obliterans in allogeneic rat lung transplantation--effectiveness of everolimus. Exp. Toxicol. Pathol. 65, 383-389.

von Suesskind-Schwendi M., Valenti V., Haneya A., Pühler T., Bewig B., Schmid C., Hirt S.W. and Lehle K.(2013b). Synergism of imatinib mesylate and everolimus in attenuation of bronchiolitis obliterans after rat LTX. Histol. Histopathol. 28, 1273-1284.

Weigt S.S., DerHovanessian A., Wallace W.D., Lynch J.P. and Belperio J.A. (2013). Bronchiolitis obliterans syndrome: the Achilles' heel of lung transplantation. Semin. Respir. Crit. Care Med. 34, 336-351.

Yuge R., Kitadai Y., Shinagawa K., Onoyama M., Tanaka S., Yasui W. and Chayama K. (2005). mTOR and PDGF pathway blockade inhibits liver metastasis of colorectal cancer by modulating the tumor microenvironment. Am. J. Pathol. 185, 399-408.

Zhou H., Latham C.W., Zander D.S., Margolin S.B. and Visner G.A. (2005). Pirfenidone inhibits obliterative airway disease in mouse tracheal allografts. J. Heart Lung Transplant. 24, 1577-1585.

Accepted December 28, 2015